Imaging in Thoracic Disease

Seong Yong Park, M.D., Ph.D.

Clinical Assistant Professor
Department of Thoracic and Cardiovascular Surgery
Yonsei University College of Medicine, Seoul, Korea

JAMA Network Open

Original Investigation | Imaging

Development and Validation of a Deep Learning–Based Automated Detection Algorithm for Major Thoracic Diseases on Chest Radiographs

Eui Jin Hwang, MD; Sunggyun Park, MS; Kwang-Nam Jin, MD; Jung Im Kim, MD; So Young Choi, MD; Jong Hyuk Lee, MD; Jin Mo Goo, MD, PhD; Jaehong Aum, PhD; Jae-Joon Yim, MD; Julien G. Cohen, MD; Gilbert R. Ferretti, MD; Chang Min Park, MD, PhD; for the DLAD Development and Evaluation Group

Abstract

IMPORTANCE Interpretation of chest radiographs is a challenging task prone to errors, requiring expert readers. An automated system that can accurately classify chest radiographs may help streamline the clinical workflow.

OBJECTIVES To develop a deep learning–based algorithm that can classify normal and abnormal results from chest radiographs with major thoracic diseases including pulmonary malignant neoplasm, active tuberculosis, pneumonia, and pneumothorax and to validate the algorithm's performance using independent data sets.

DESIGN, SETTING, AND PARTICIPANTS This diagnostic study developed a deep learning–based algorithm using single-center data collected between November 1, 2016, and January 31, 2017. The algorithm was externally validated with multicenter data collected between May 1 and July 31, 2018. A total of 54 221 chest radiographs with normal findings from 47 917 individuals (21 556 men and 26 361 women; mean [SD] age, 51 [16] years) and 35 613 chest radiographs with abnormal findings from 14 102 individuals (8373 men and 5729 women; mean [SD] age, 62 [15] years) were used to develop the algorithm. A total of 486 chest radiographs with normal results and 529 with abnormal results (1 from each participant; 628 men and 387 women; mean [SD] age, 53 [18] years) from 5 institutions were used for external validation. Fifteen physicians, including nonradiology physicians, board-certified radiologists, and thoracic radiologists, participated in observer performance testing. Data were analyzed in August 2018.

EXPOSURES Deep learning–based algorithm.

MAIN OUTCOMES AND MEASURES Image-wise classification performances measured by area under the receiver operating characteristic curve; lesion-wise localization performances measured by area under the alternative free-response receiver operating characteristic curve.

RESULTS The algorithm demonstrated a median (range) area under the curve of 0.979 (0.973-1.000) for image-wise classification and 0.972 (0.923-0.985) for lesion-wise localization; the algorithm demonstrated significantly higher performance than all 3 physician groups in both image-wise classification (0.983 vs 0.814-0.932; all $P < .005$) and lesion-wise localization (0.985 vs 0.781-0.907; all $P < .001$). Significant improvements in both image-wise classification (0.814-0.932 to 0.904-0.958; all $P < .005$) and lesion-wise localization (0.781-0.907 to 0.873-0.938; all $P < .001$) were observed in all 3 physician groups with assistance of the algorithm.

CONCLUSIONS AND RELEVANCE The algorithm consistently outperformed physicians, including thoracic radiologists, in the discrimination of chest radiographs with major thoracic diseases,

Key Points

Question Can a deep learning–based algorithm accurately discriminate abnormal chest radiograph results showing major thoracic diseases from normal chest radiograph results?

Findings In this diagnostic study of 54 221 chest radiographs with normal findings and 35 613 with abnormal findings, the deep learning–based algorithm for discrimination of chest radiographs with pulmonary malignant neoplasms, active tuberculosis, pneumonia, or pneumothorax demonstrated excellent and consistent performance throughout 5 independent data sets. The algorithm outperformed physicians, including radiologists, and enhanced physician performance when used as a second reader.

Meaning A deep learning–based algorithm may help improve diagnostic accuracy in reading chest radiographs and assist in prioritizing chest radiographs, thereby increasing workflow efficacy.

+ Supplemental content

Author affiliations and article information are listed at the end of this article.

Figure 2. Representative Case From the Observer Performance Test (Malignant Neoplasm)

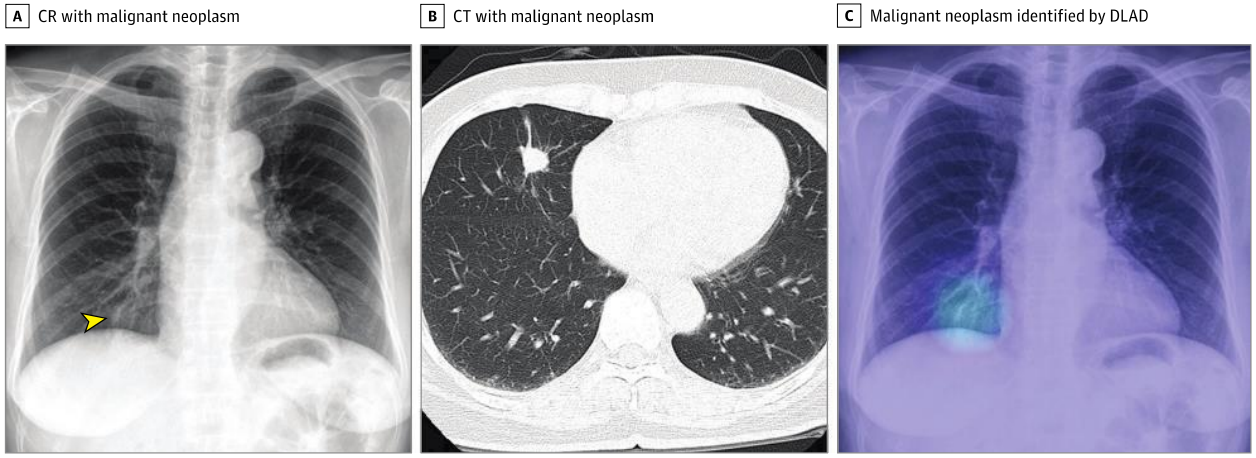

A, The chest radiograph (CR) shows nodular opacity at the right lower lung field (arrowhead), which was initially detected by 2 of 15 observers. B, The corresponding computed tomographic (CT) image reveals a nodule at the right middle lobe. C, The deep learning–based automatic detection algorithm (DLAD) correctly localized the lesion (probability score, 0.291). Four observers additionally detected the lesion after checking the output.

Figure 3. Representative Case From the Observer Performance Test (Pneumonia)

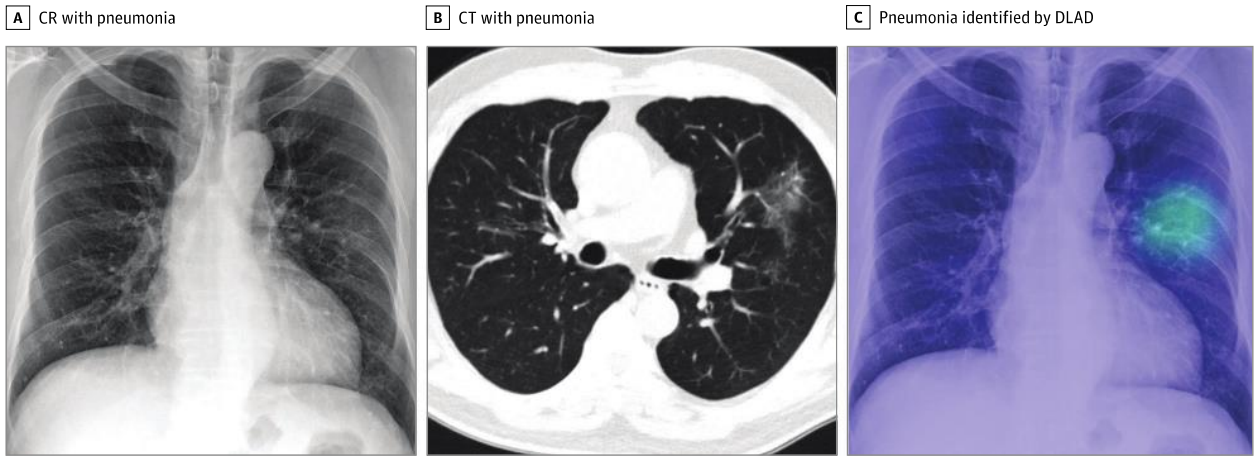

A, The chest radiograph (CR) shows subtle patchy increased opacity at the left middle lung field, which was initially missed by all 15 observers. B, The corresponding computed tomographic (CT) image shows patchy ground glass opacity at the left upper lobe. C, The deep learning–based automatic detection algorithm (DLAD) correctly localized the lesion (probability score, 0.371). Seven observers correctly detected the lesion after checking the result.

Figure 1. Results of External Validation Tests and Observer Performance Tests

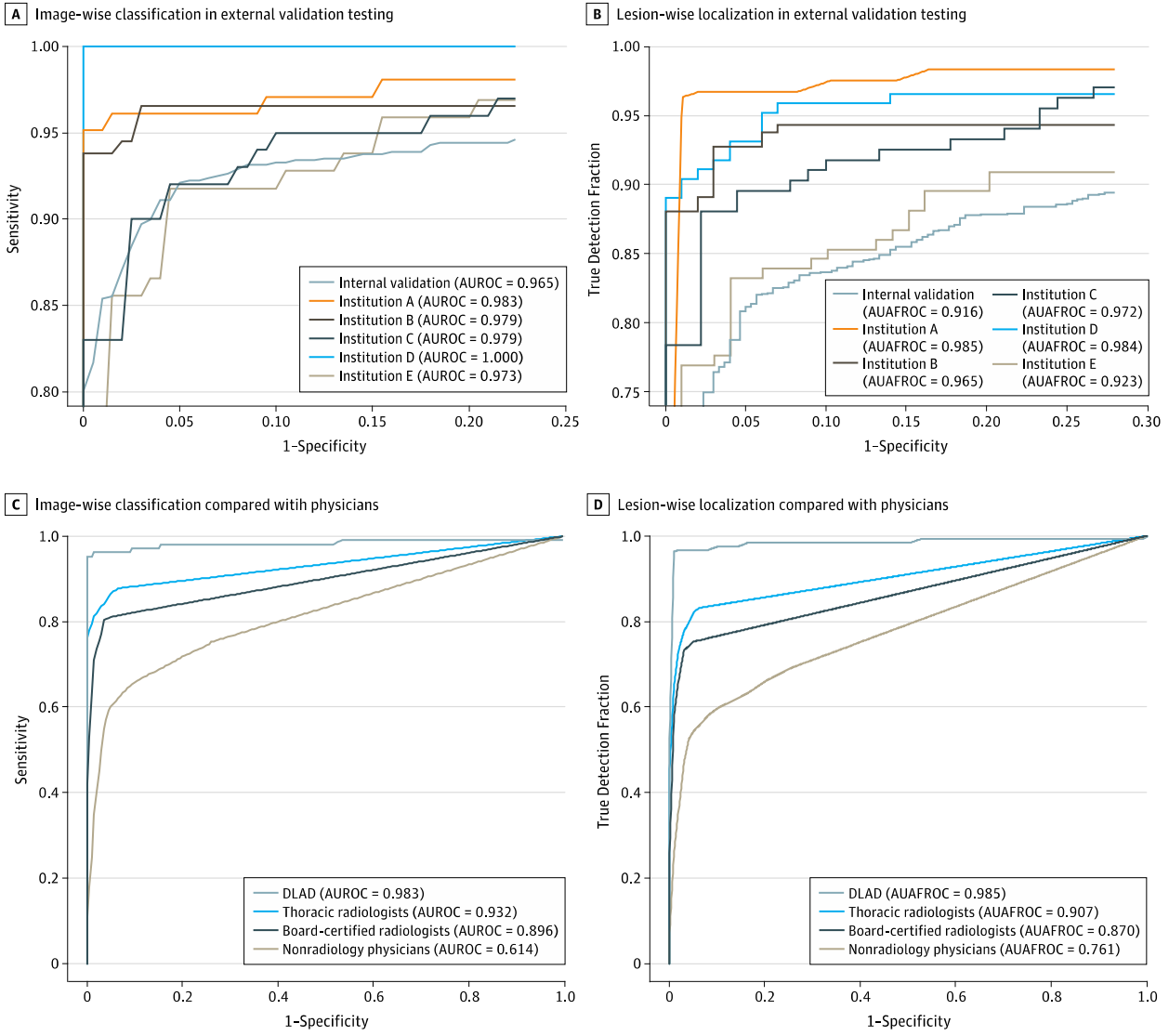

The deep learning–based automatic detection algorithm (DLAD) showed consistently high image-wise classification (area under the receiver operating characteristic curve [AUROC], 0.973-1.000) (A) and lesion-wise localization (area under the alternative free-response receiver operating characteristic curve [AUAFROC], 0.923-0.985) (B) performances in external validation tests. In comparison of performance with physicians, the DLAD showed significantly high classification (AUROC, 0.983 vs 0.814-0.932) (C) and localization (AUAFROC, 0.985 vs 0.781-0.907) (D) performances than all observer groups.

많이 사용하는 영상

- Chest X-ray
- Chest CT, abdomen CT
- PET
- MRI
- Esophagography

- Bed-side ultrasound

Radiologic Density Contrast

- X-ray absorption coefficient
  - Metal density ; bone, calcified LN
  - Water density ; almost all solid organs
  - Fat density ; subcutaneous, mesenteric retroperitonal fat
  - Air density ; lung, hollow viscus

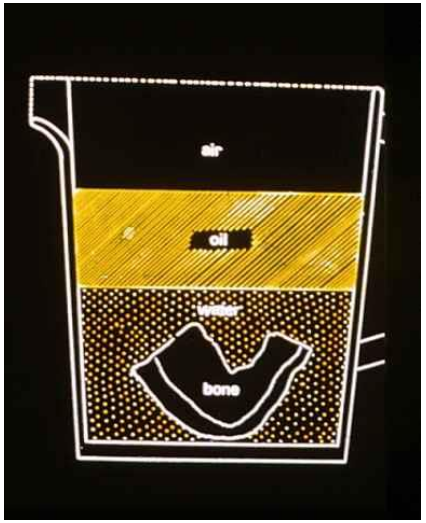

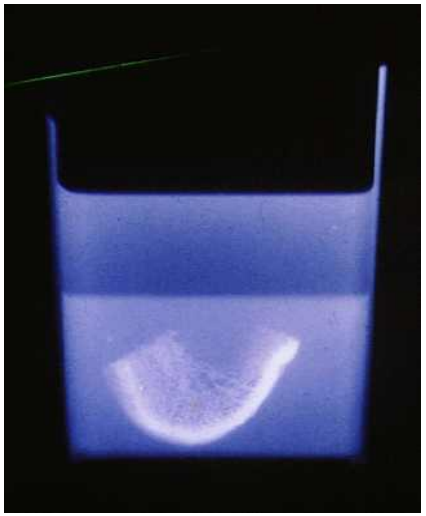

- Hounsfield Unit
  - X선이 몸을 투과할대 부위별 밀도에 의해 흡수되는 정도를 상대적으로 표현
  - Water 0, Bone 1000, air -1000

Radiologic Density Contrast

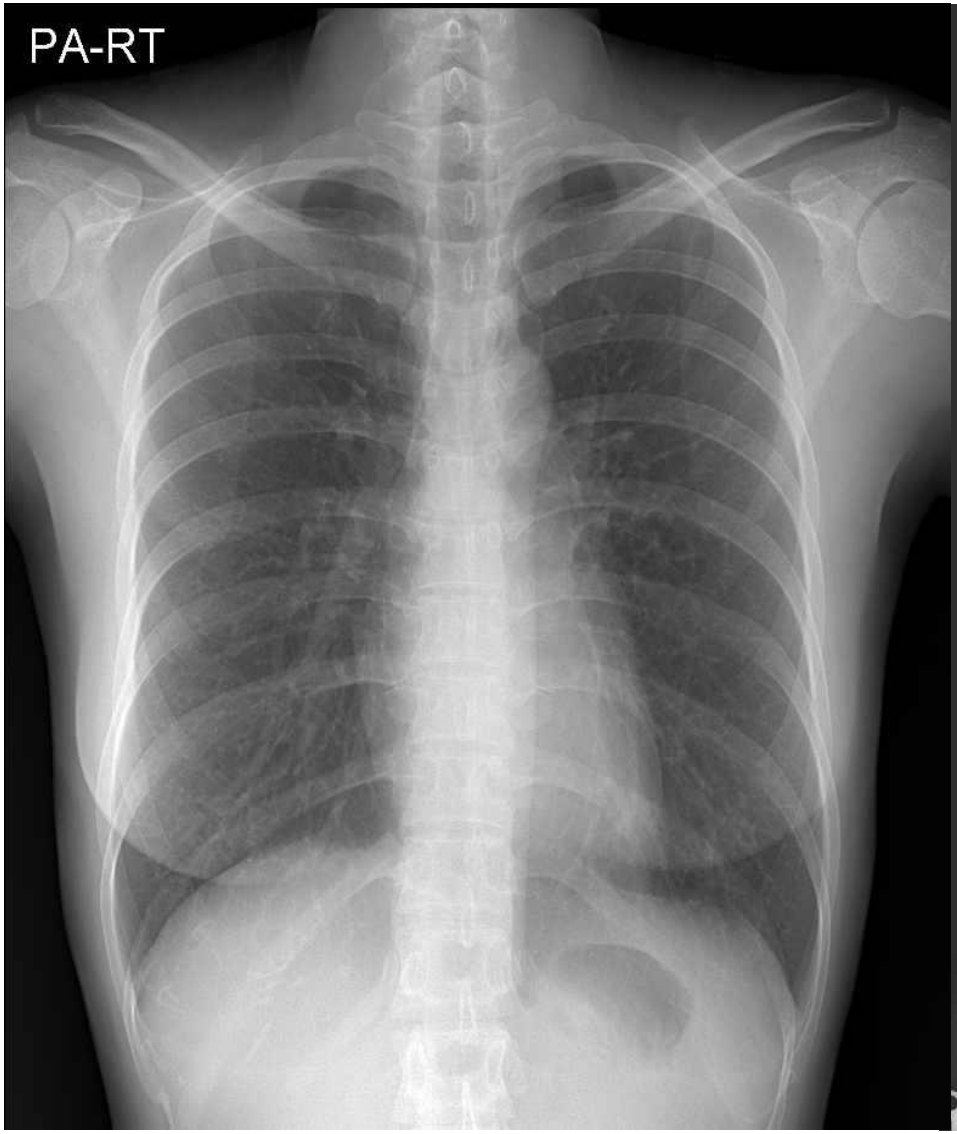

Radiologic Density Contrast

Mediastinal window

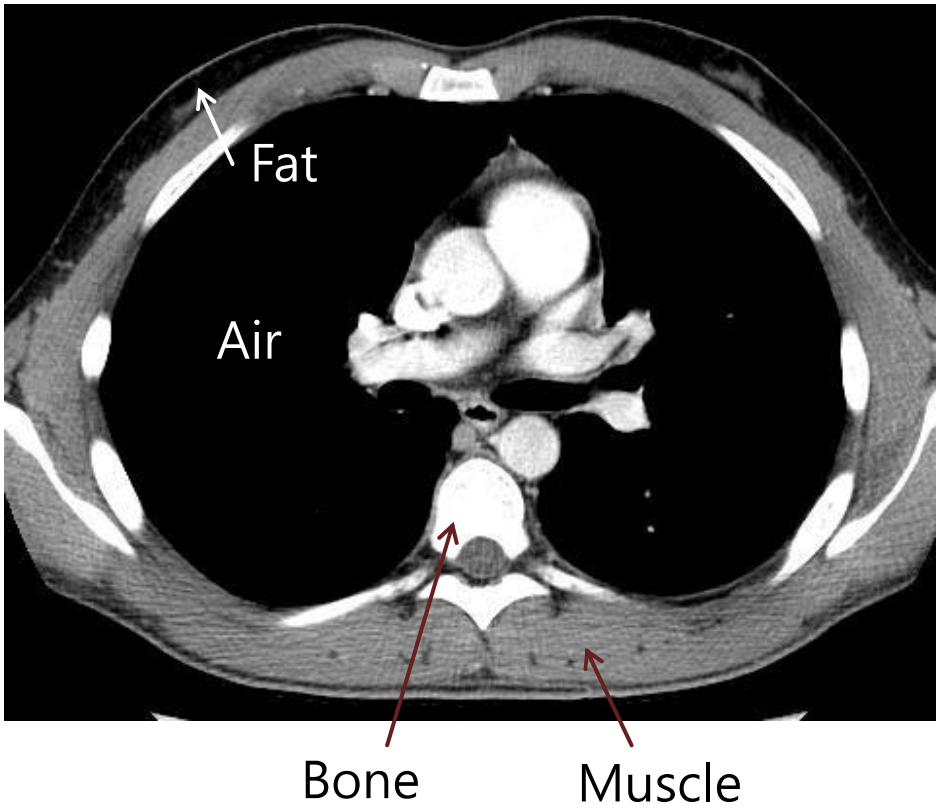

Lung window

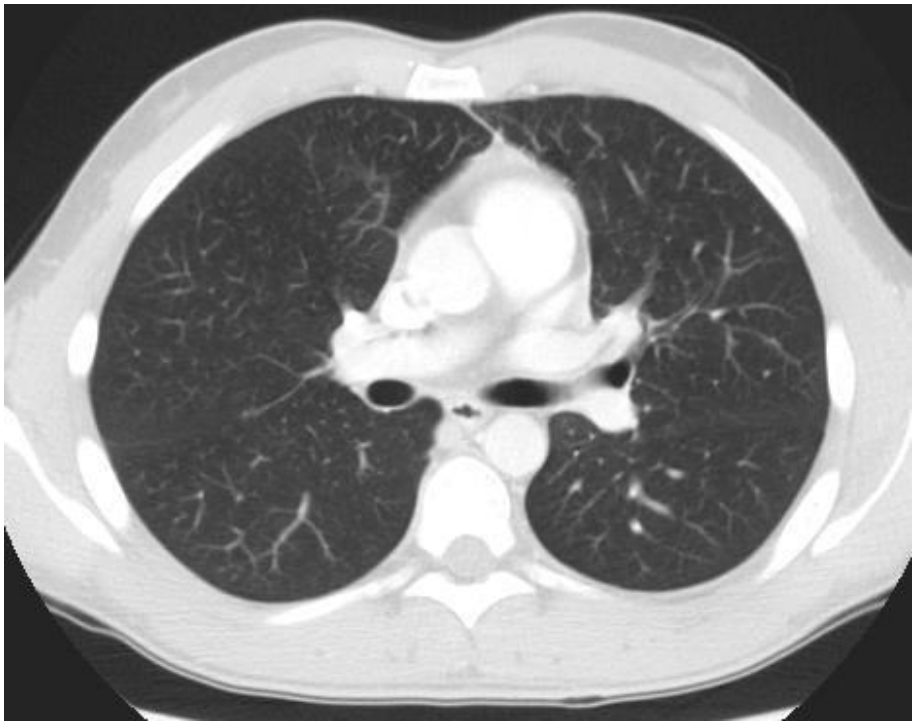

Plane

- Axial; 위에서 아래로 촬영
- Coronal; 정면에서 촬영
- Sagittal; 측면에서 촬영

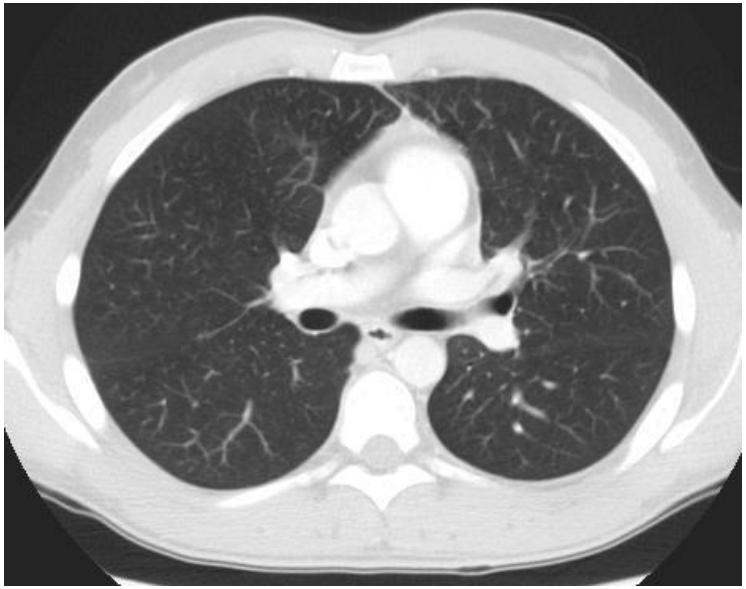

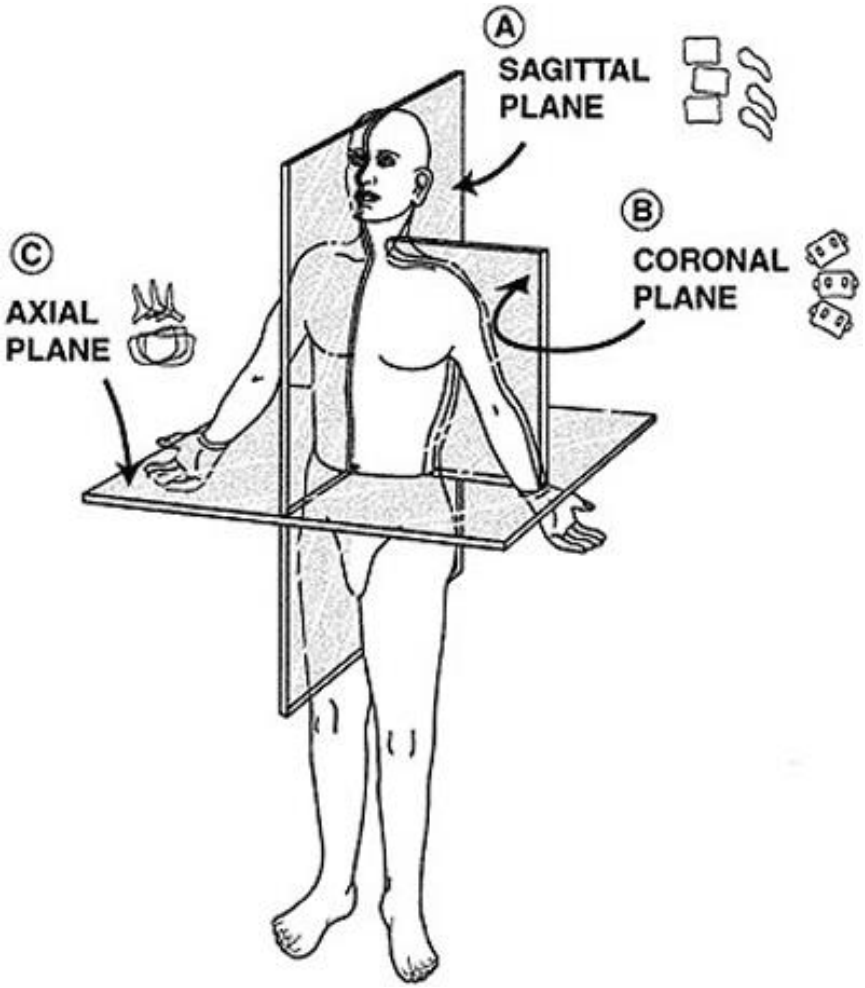

X-ray 촬영 방법

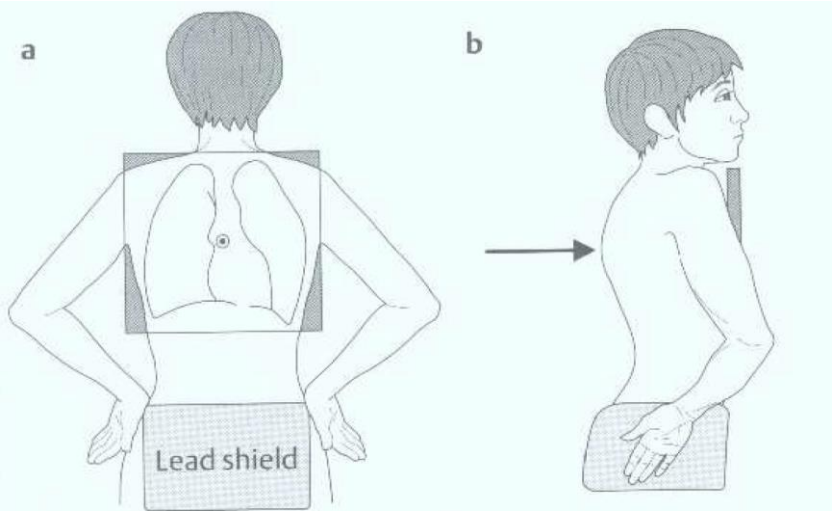

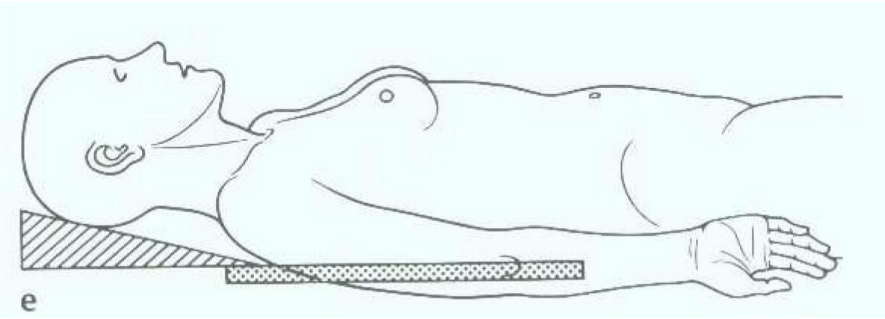

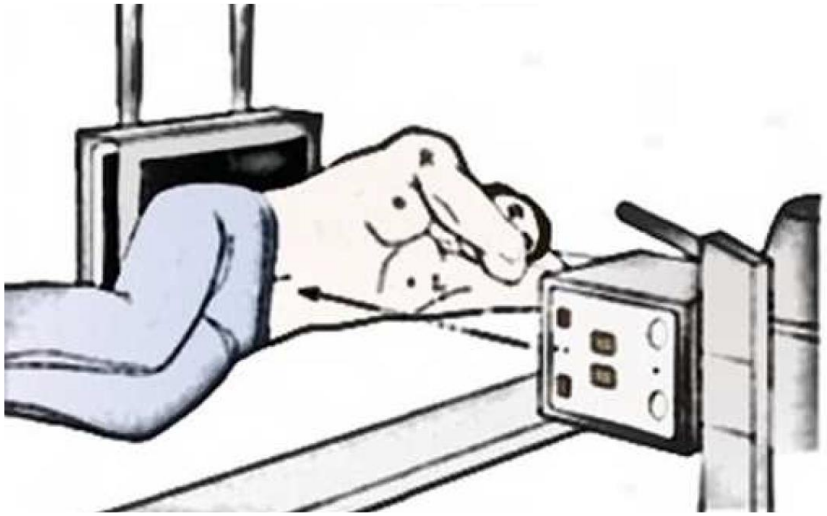

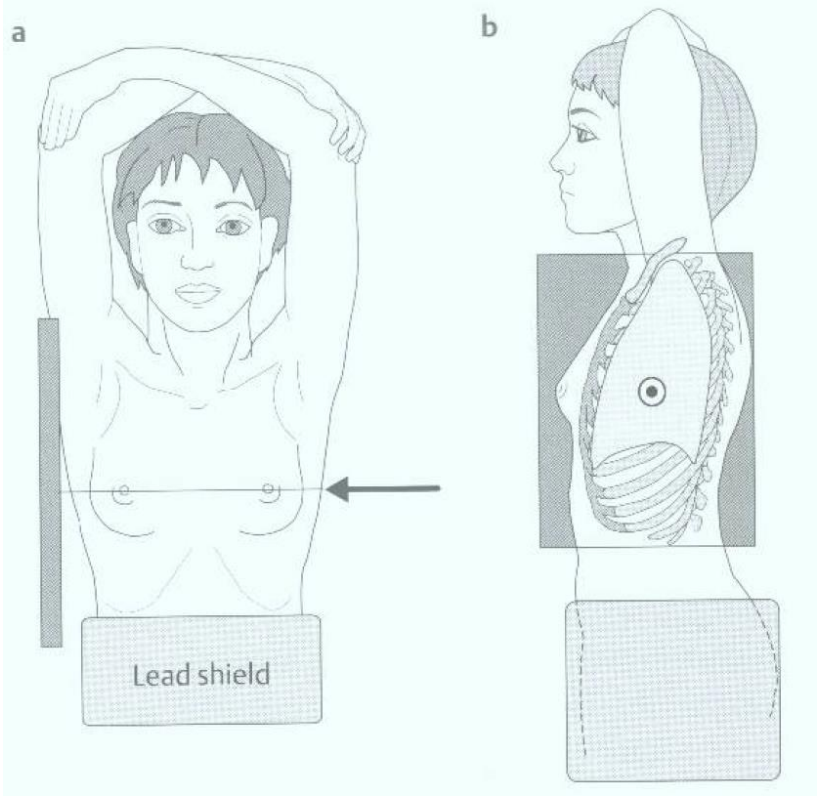

Chest X-ray

- Pneumothorax, pleural effusion
- Atelectasis
- Infiltration
- Mass lesion
- Rib fracture
- Central line, chest tube 및 기타 삽관들의 위치 확인, 위치의 변화
  - Tracheostomy, L-tube, drain….

- 항상 이전 X-ray와 비교해야 한다

- Density를 잘 조정해야 한다

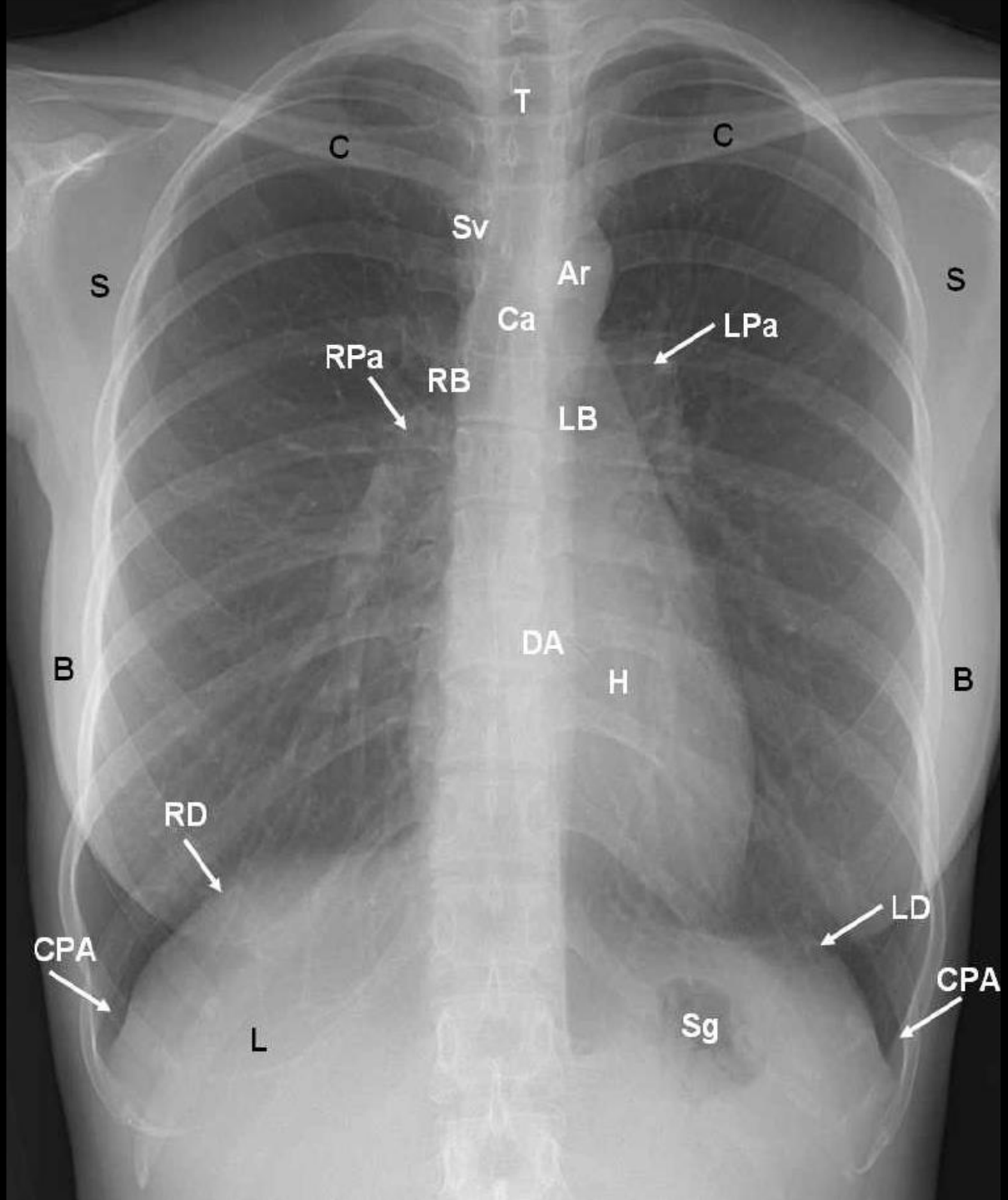
T
C
C
Sv
S
Ar
S
Ca
LPa
RPa
RB
LB
DA
B
H
B
RD
LD
CPA
CPA
L
Sg

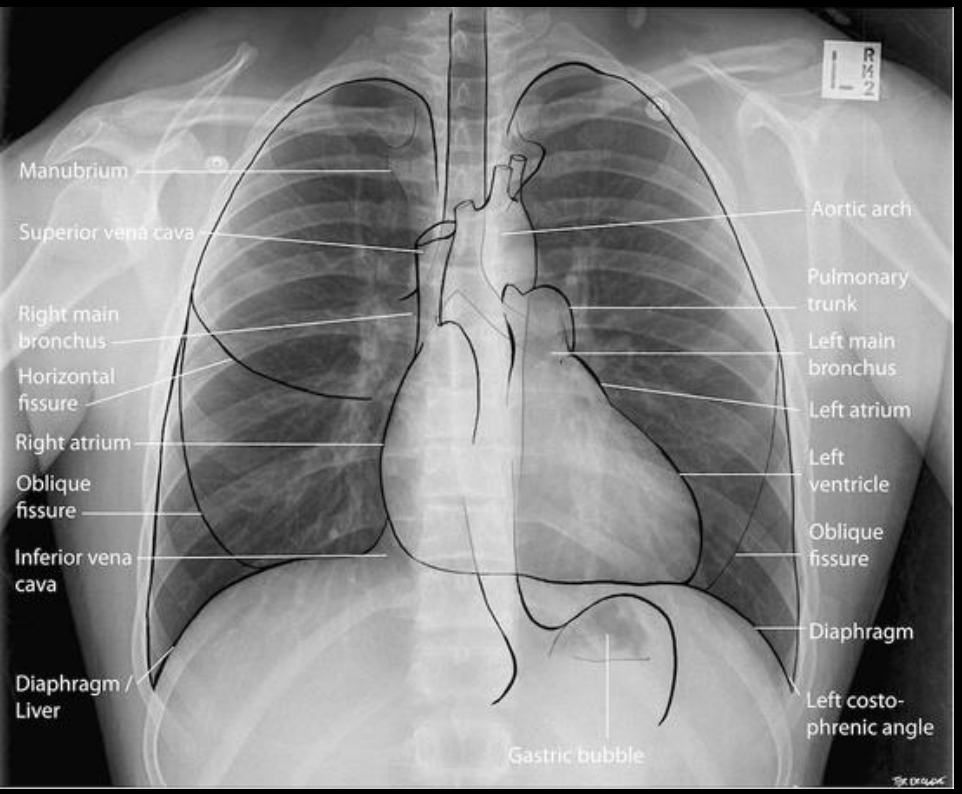
Manubrium
Superior vena cava
Right main bronchus
Horizontal fissure
Right atrium
Oblique fissure
Inferior vena cava
Diaphragm / Liver
Aortic arch
Pulmonary trunk
Left main bronchus
Left atrium
Left ventricle
Oblique fissure
Diaphragm
Left costo-phrenic angle
Gastric bubble

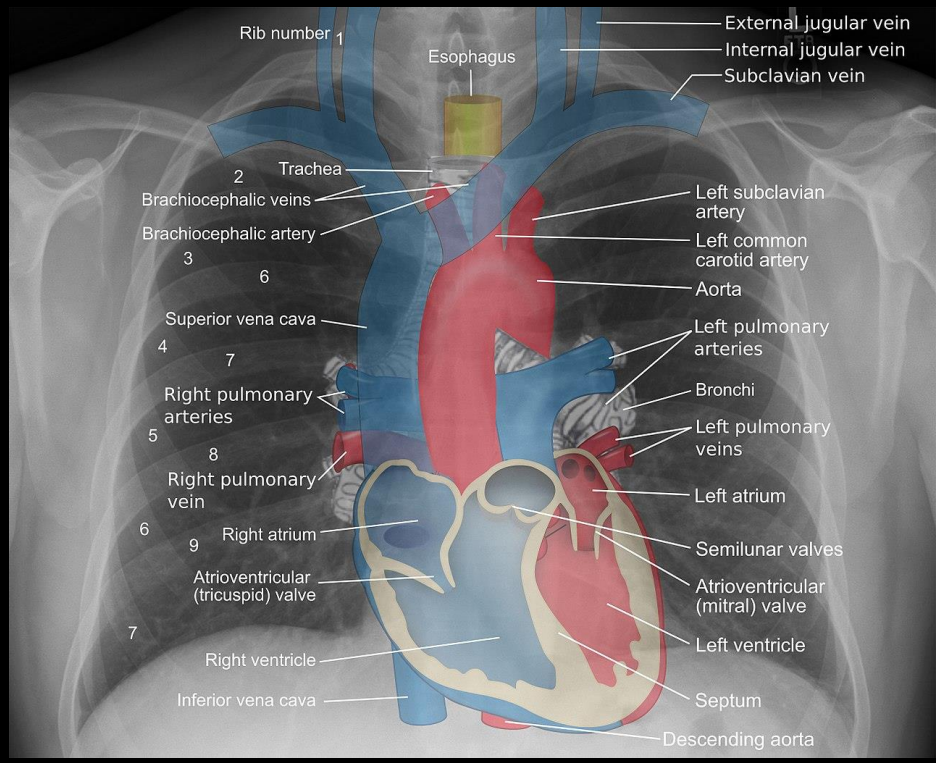
Rib number 1
Esophagus
External jugular vein
Internal jugular vein
Subclavian vein
2
Trachea
Brachiocephalic veins
Brachiocephalic artery
3
6
Superior vena cava
4
7
Right pulmonary arteries
5
8
Right pulmonary vein
6
9
Right atrium
Atrioventricular (tricuspid) valve
7
Right ventricle
Inferior vena cava
Left subclavian artery
Left common carotid artery
Aorta
Left pulmonary arteries
Bronchi
Left pulmonary veins
Left atrium
Semilunar valves
Atrioventricular (mitral) valve
Left ventricle
Septum
Descending aorta


R

Chest CT

- Most important imaging modality in thoracic disease (backbone of thoracic imaging)

- Contrast
  - Iodine dye
  - Can cause the renal failure

- 종류
  - Chest CT contrast vs. noncontrast
  - Chest HR CT
  - Pulmonary CT
  - Aorta CT

Chest CT

- Axial, coronal, sagittal view를 모두 확인

- Lung setting, mediastinal setting
- Mediastinal setting으로 먼저 본 후, lung setting으로 바꾸어서 본다
- Setting을 바꿔가면서 병변의 변화가 있는지 살펴본다

- 양측 폐를 동시에 보지 말고, 한쪽을 먼저 보고 반대쪽을 다시 보도록

- 조직의 Hounsfield Unit, contrast enhancement 여부도 중요한 단서가 된다

Chest CT

- CT 이미지의 thickness를 확인할 것
- Chest X-ray 가 애매하면 항상 CT를 찍어본다 (noncon이라도)
- Leak이 의심되는 경우는 barium등을 먹이고 CT를 촬영해볼 수 있다
- Nodule과 vessel이 헷갈릴 경우는 위 아래로 이어지는 병변인지 확인한다

PET

- Glucose uptake of cells
- Physiologic uptake, inflammation
- Tracer; FDG, other tracers (ex. 11c-MET for parathyroid)
- Parameters
  - SUV (standardized uptake value)max, SUVmean
  - MTV (metabolic tumor volume)
  - TLG (Total lesion glycolysis) = SUVmean x MTV

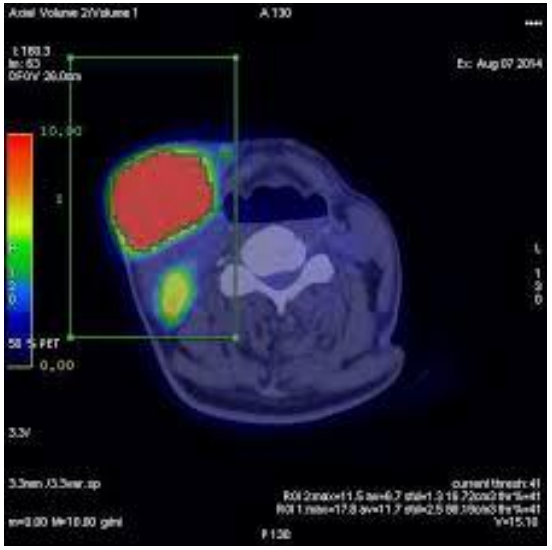

Biography

Dr. Zang Hee Cho graduated Seoul National University and did Ph.D in Applied physics at Uppsala University, Sweden.

Professor Cho has been faculty of University of California, Los Angeles, Columbia University, and University of California, Irvine. Professor Cho is currently Distinguished Research Fellow at the AICT, Seoul National University.

Professor Cho in the pioneer of CT, PET, and MRI and developed world's first PET scanner in 1975 while he was at UCLA. Among many awards and honors, Professor Cho elected as a member of US National Academy of Medicine in 1977.

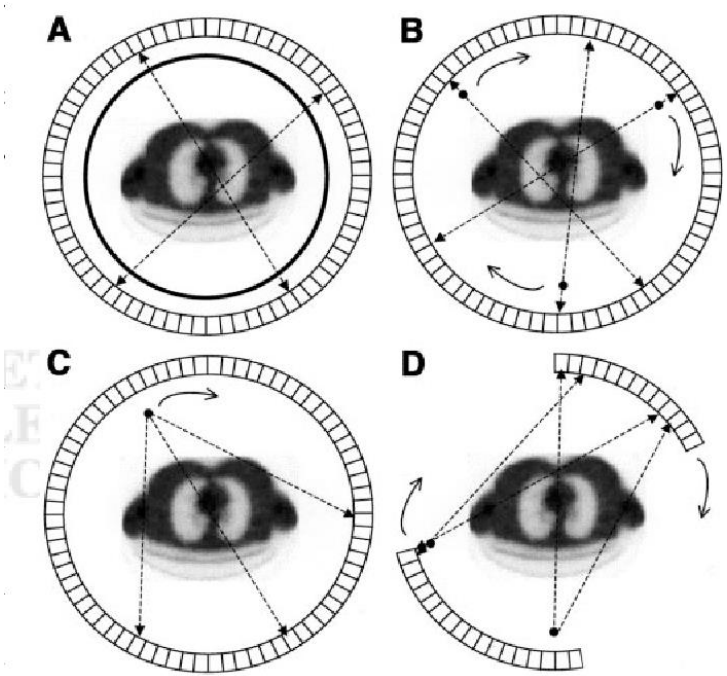

PET

- Brain 병변은 확실히 알 수 없다
- 크기가 작은 병변은 FDG uptake이 높아도 PET에서는 잘 보이지 않을 수 있다; 7mm ~ 1cm 이상은 되어야 확인 가능
- PET/CT 상에서 두 이미지가 완벽하게 일치하지 않을 수 있다; breathing, normal GI motility
- 감염성 질환은 암과 오인될 수 있다
- 그래도 현재로서 preoperative staging에 가장 정확한 imaging tool 이다

CT Transaxials

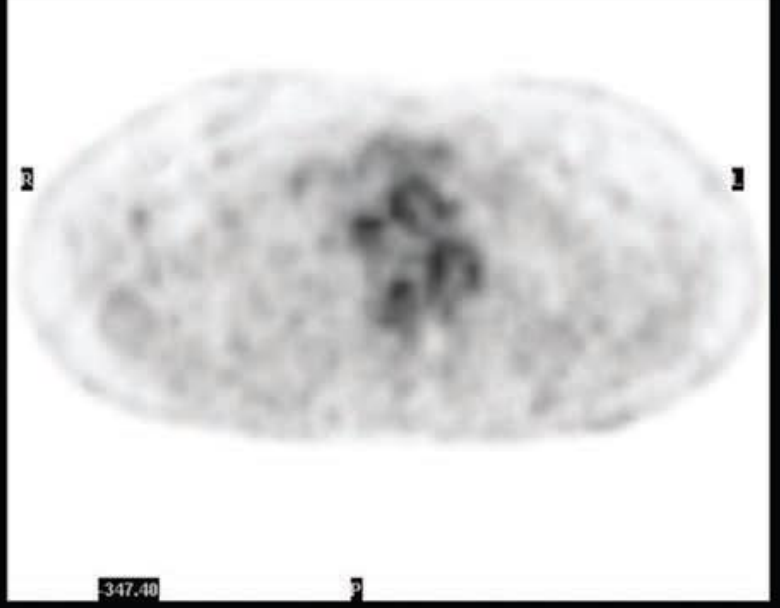

PET Transaxials

Fused Transaxials

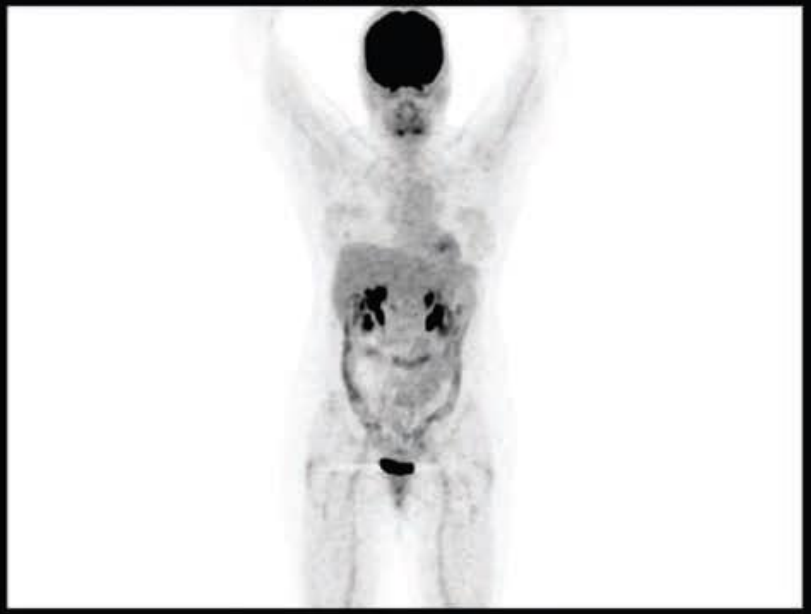

MIP Navigate

MRI

- Useful situation
  - Brachial plexus invasion
  - Spinal cord invasion
  - Brain metastasis
  - Pancoast tumor, thoracic outlet syndrome, mesothelioma, adrenal mass
- Not useful situation
  - Invasion of aorta or trachea
- 어떤 MRI를 촬영해야 하는지는 영상의학과 전문의와 반드시 상의

MRI in esophageal cancer

- Chest MR with cine, dynamic, T2-SSH, b-FFE, THRIVE, DWI, T2-STIR
- Asymmetric enhancing wall thickening of upper esophagus, suggestive of esophageal cancer.
- Ill-defined margin between posterior tracheal membrane and esophageal mass, suspicious of invasion.
- Suspicious of azygos vein invasion.
- No definite aortic invasion.
- r/o metastatic LN in the Lt. highest mediastinum.
- Fibrosis with granulomas in both upper lobes, probably Tbc sequelae.

Pneumothorax

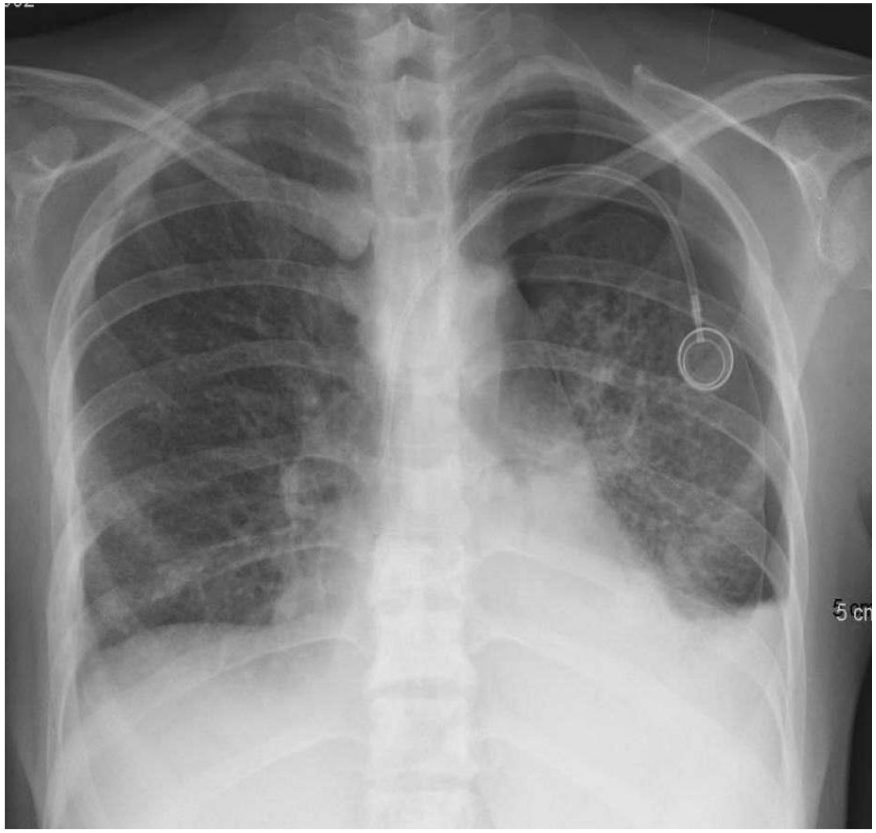

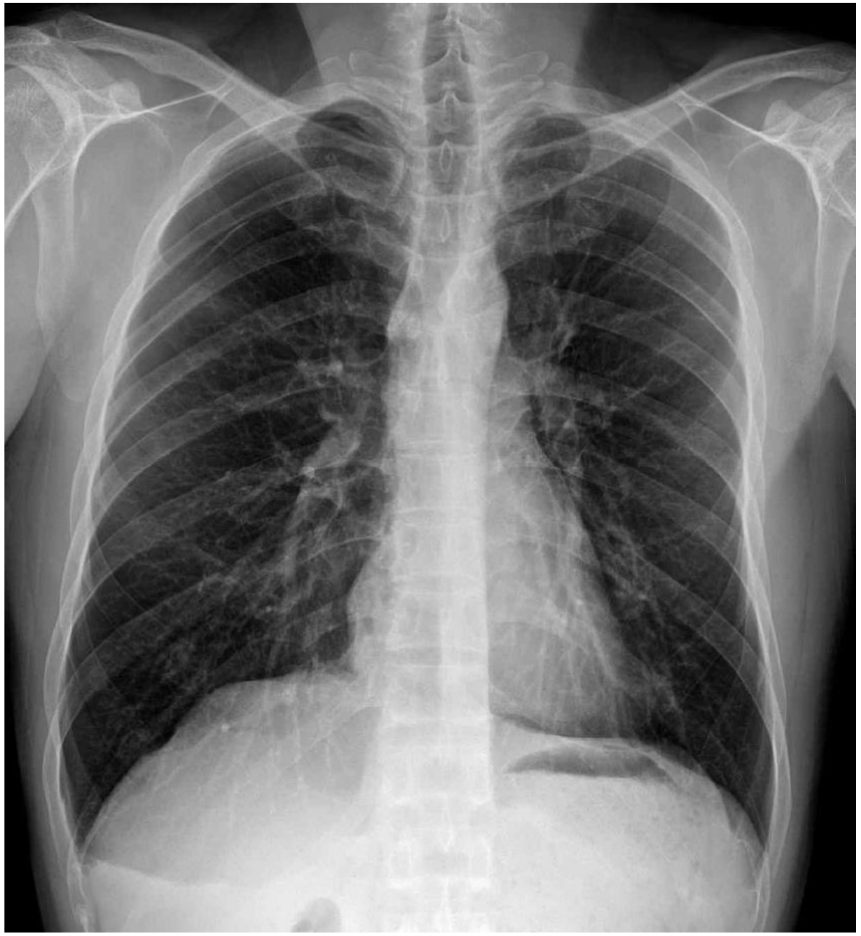

Pneumothorax in chest AP

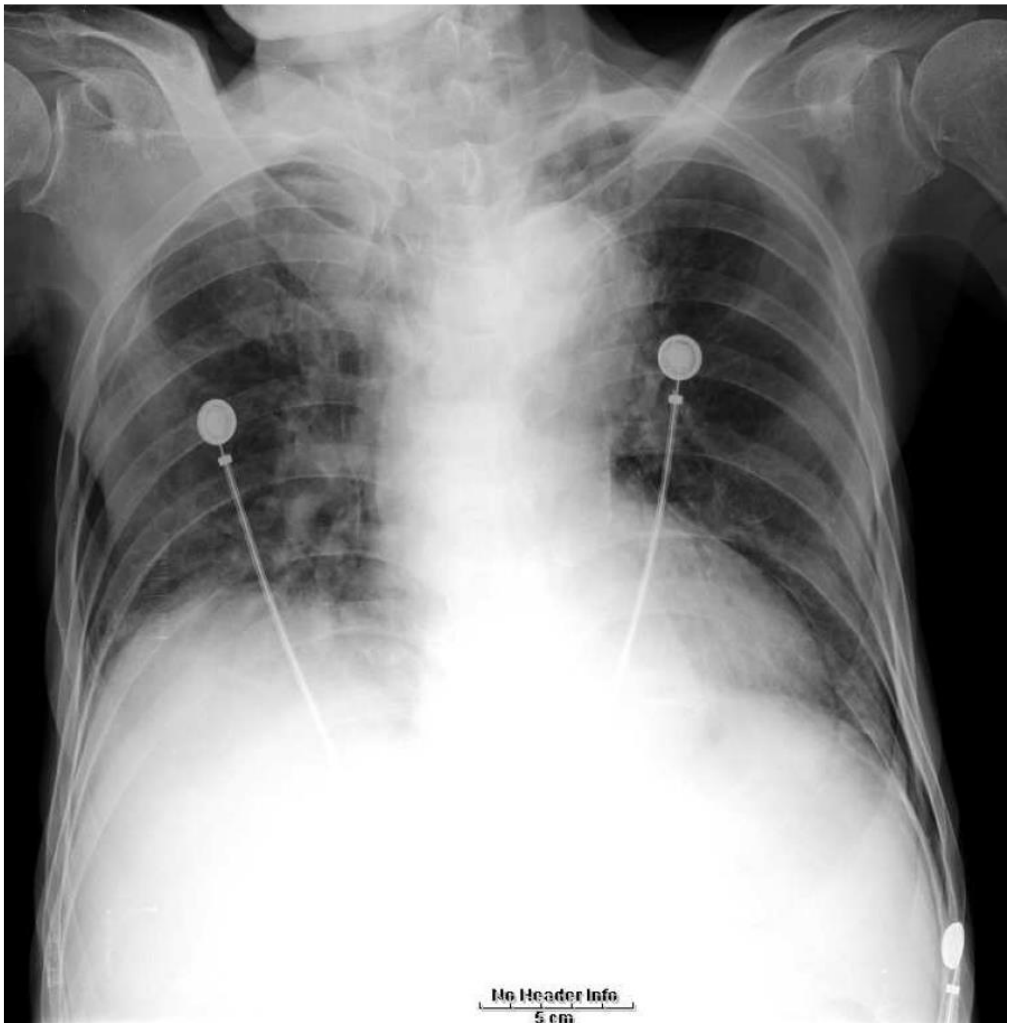

- 앙아위에서는 약 500cc 정도의 공기가 있어야 진단이 가능
- 공기는 주로 내전방부, 폐하부, 늑골횡경막각에 존재
- 늑골횡경막각, 심장횡경막각의 방사선 투과성 증가
- 심장 윤곽이 분명해짐

Skinfold

- 기흉으로 오인될 가능성 있음
- Line 바깥에 존재하는 혈관음영
- Line이 흉벽까지 연장

Pleural effusion

- Meniscus sign: 위로 오목한 fluid level
- CPA의 blunting
- 75ml → posterior CPA blunting → lateral view
- 150ml → Lateral CPA blunting → chest PA
- 50ml → Lateral decubitus view (fluid shift)
- Meniscus가 4번째 늑골의 전방부에 도달하면 약 1,000ml

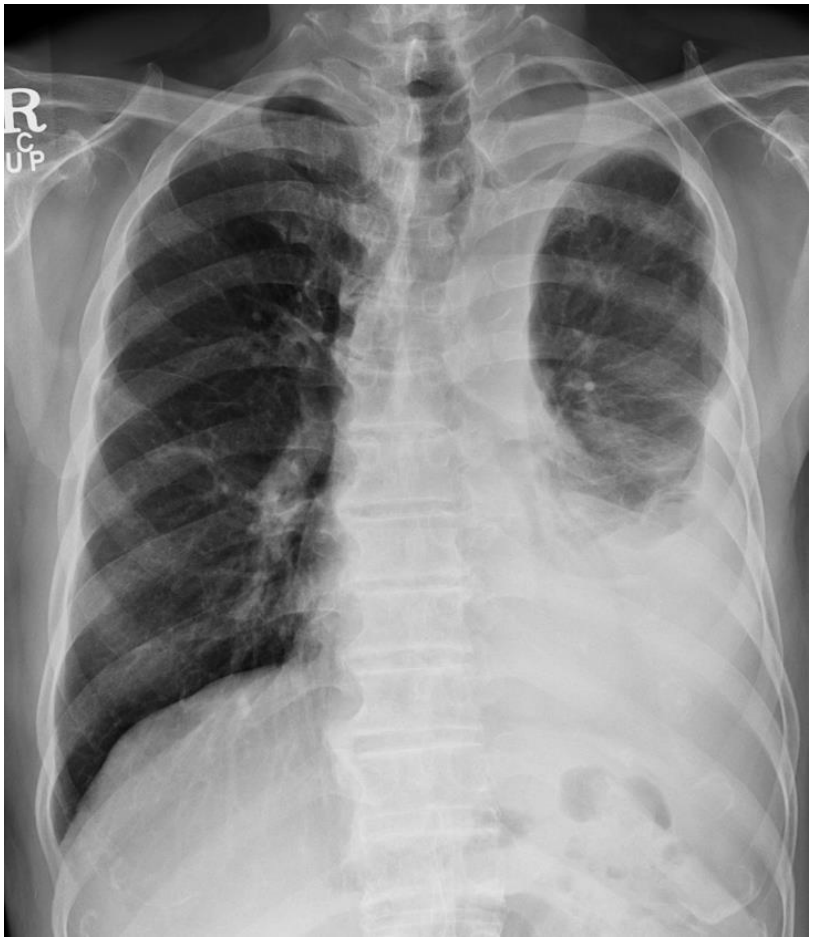

Pleural effusion at chest AP

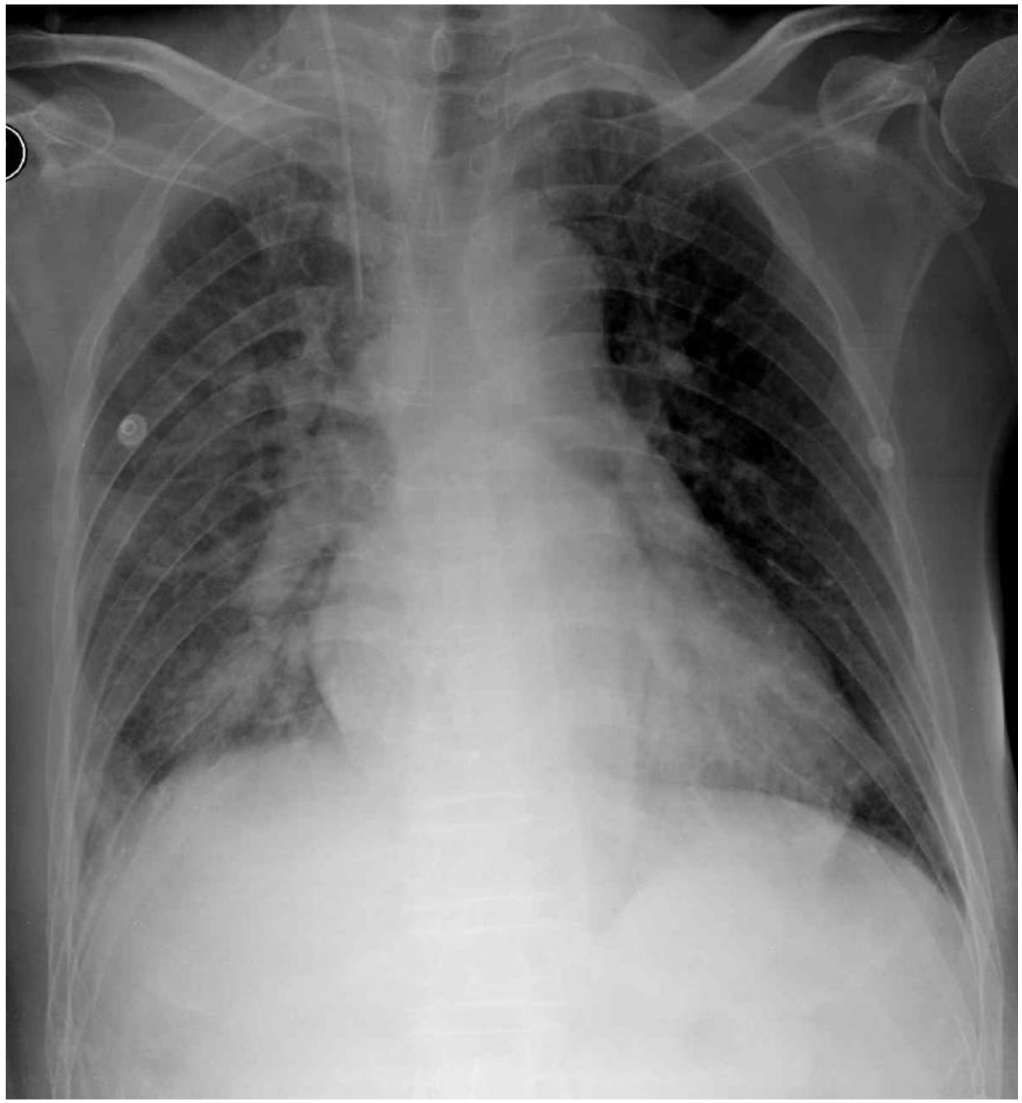

- 흉수가 폐 뒤쪽에 고임
- 소견
  - 폐음영의 전반적인 증가
  - 횡격막 윤곽의 둔화
  - 두꺼워진 폐첨

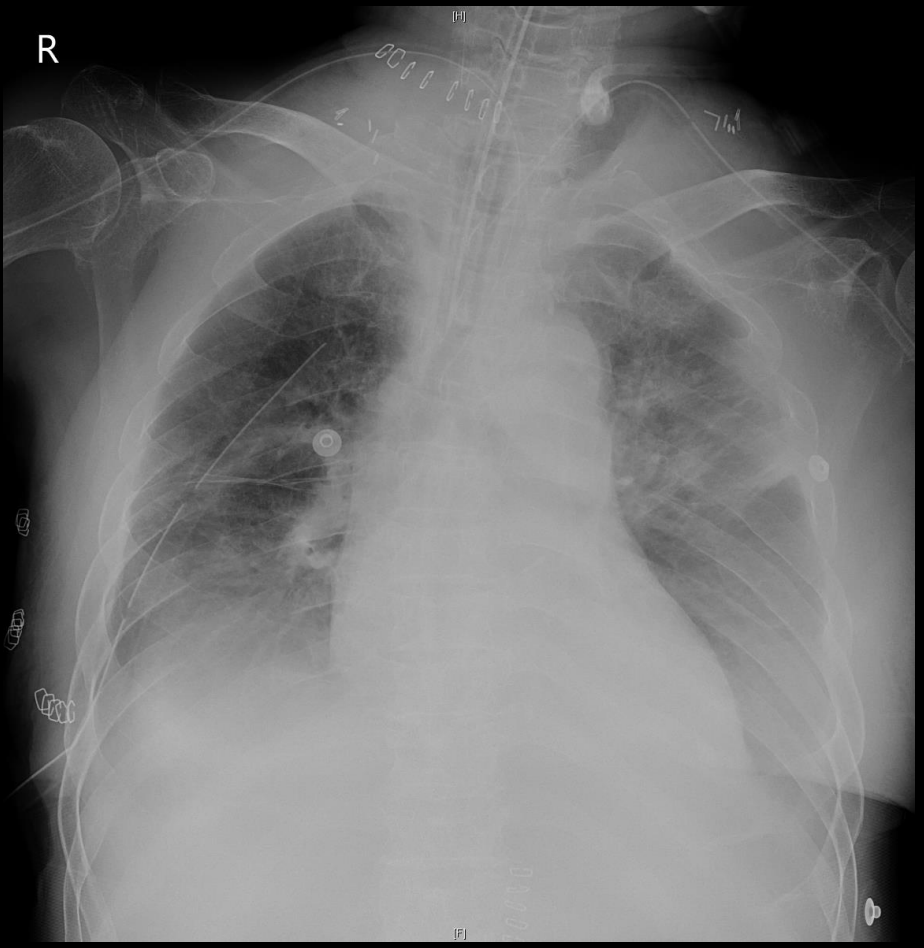
R
[H]
[F]


[A]
[P]

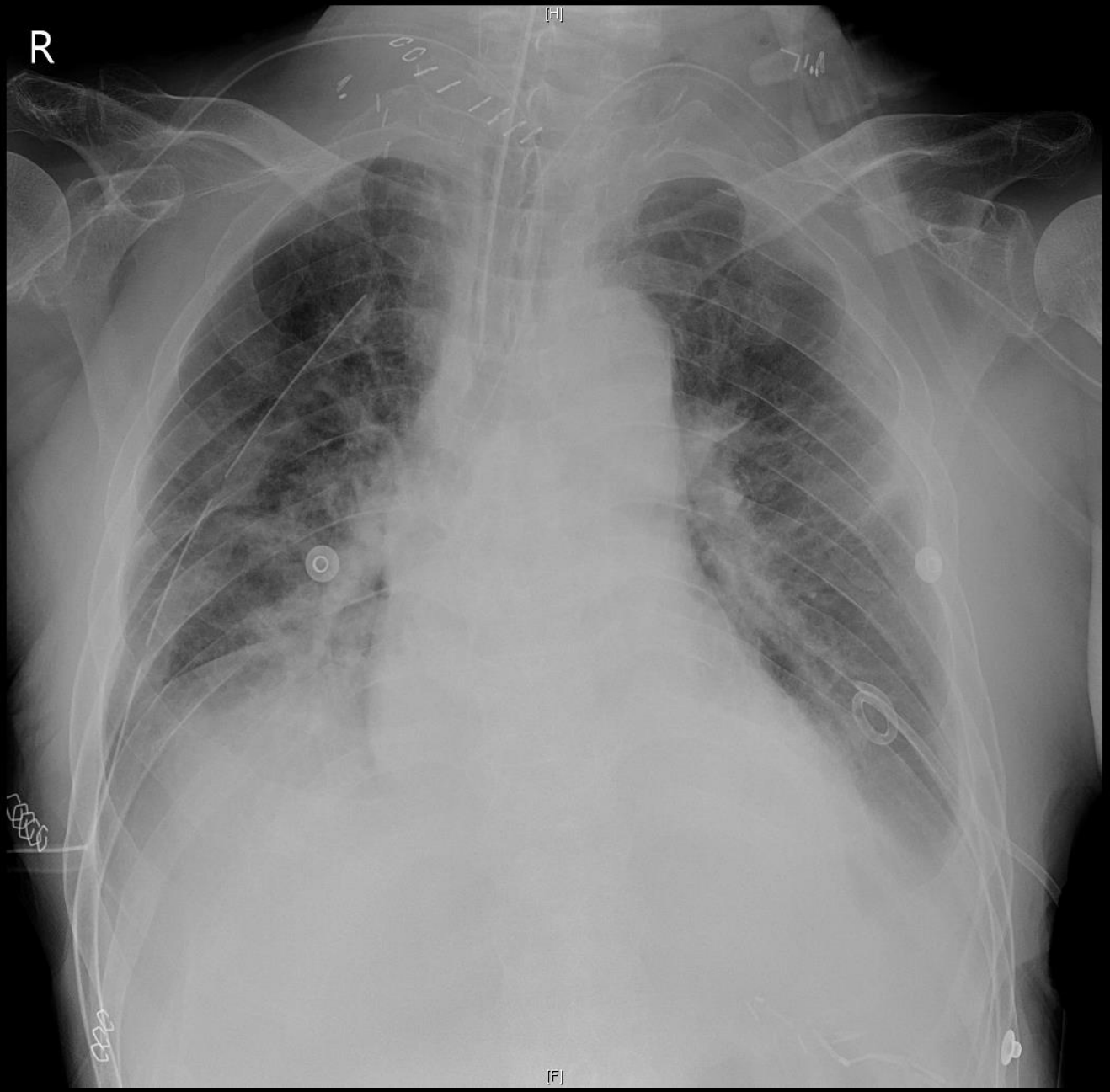
R
[H]
[F]

Effusion vs. atelectasis

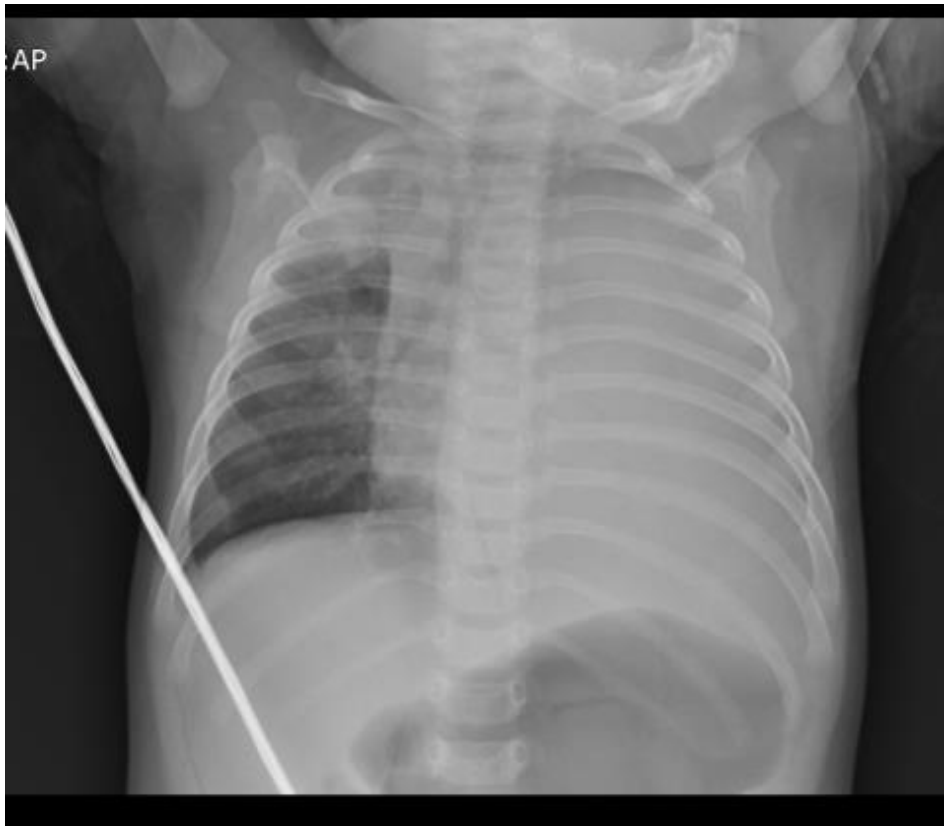

Pleural effusion at chest CT

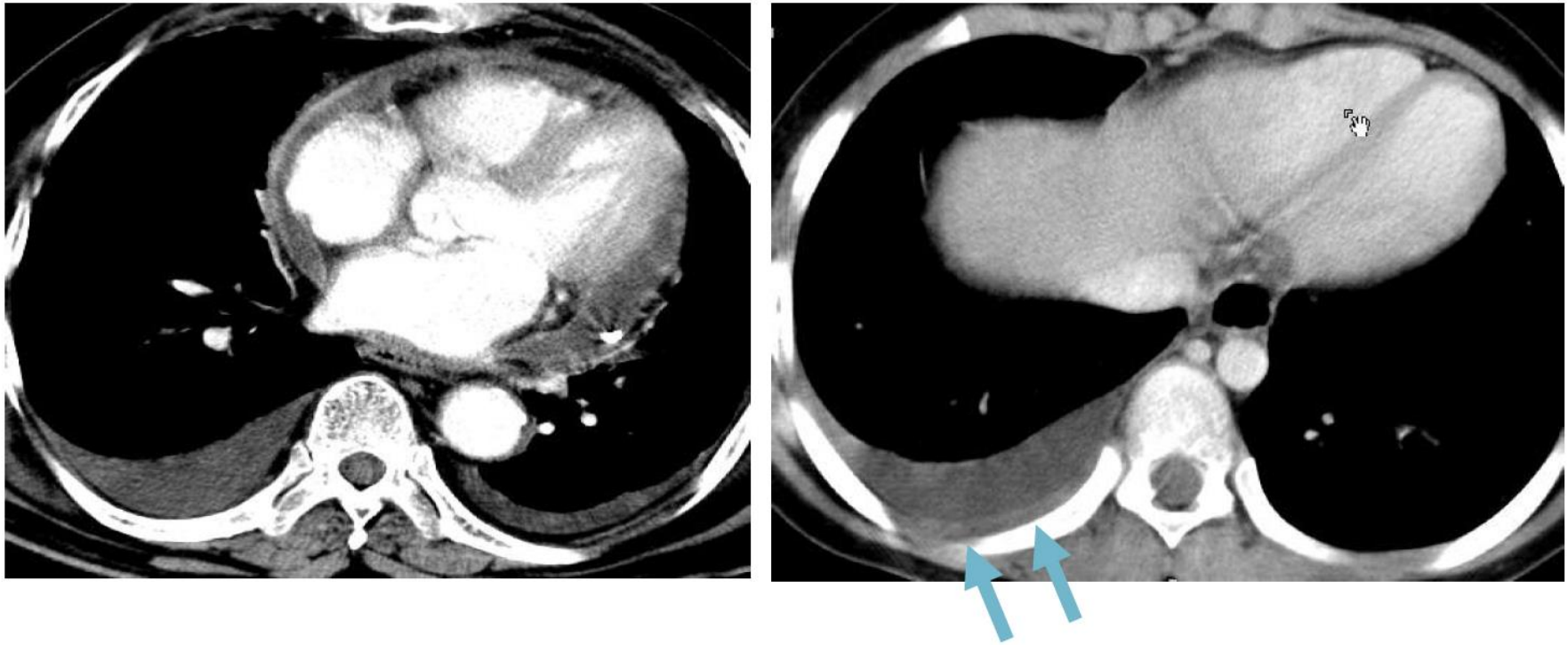

Empyema sac

Empyema sac

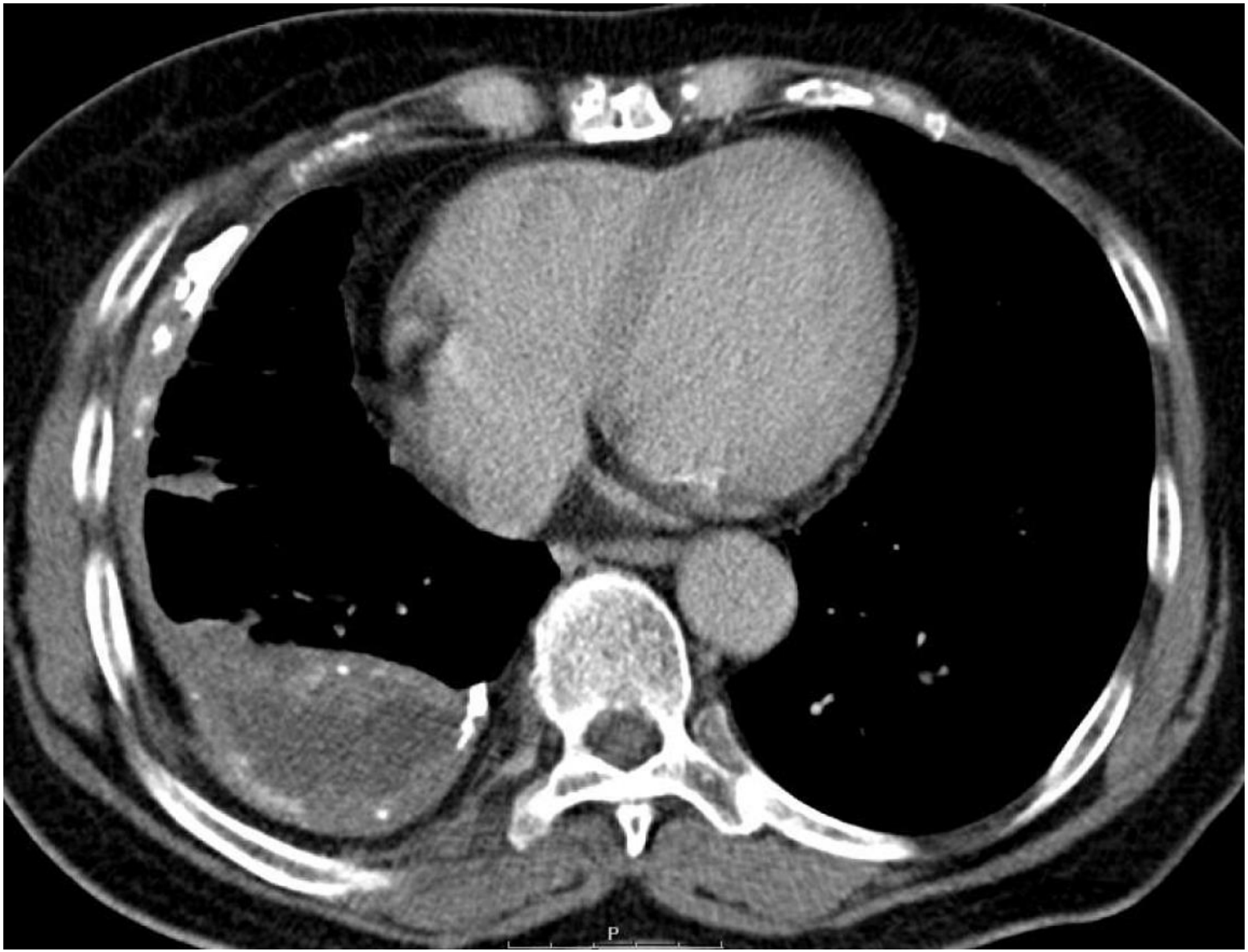

Solitary pulmonary nodule

Table 3-2

DIFFERENTIAL DIAGNOSIS FOR SOLITARY PULMONARY NODULES

NODULE ETIOLOGY	DISTINGUISHING CHARACTERISTICS
Granuloma	Smooth margins Solid or lamellated calcifications
Carcinoid	Lobulated margins Dystrophic, eccentric calcifications
Hamartoma	Lobulated margins Calcifications appear in rings or arcs Fat
AVM	Lobulated margins Infrequent calcification (vascular) Feeding/draining vessels
Lung cancer	Spiculated, lobulated, or smooth margins Dystrophic calcifications Large lesions with necrosis Cavitation in squamous cell carcinoma and adenocarcinoma
AIS/MIA	≤5 mm of atypical adenomatous hyperplasia Ground-glass opacity Well-demarcated margins Part-solid nodule Cystic spaces Focal extensions to pleura Very slow growth
Solid pulmonary metastasis	Nonspecific, although may have appearance characteristic of primary tumor

AVM, arteriovenous malformation; AIS/MIA, adenocarcinoma in situ/minimally invasive carcinoma.

Mediastinal mass

Table 3-3

DIFFERENTIAL DIAGNOSIS OF MEDIASTINAL MASSES

MASS	DIFFERENTIAL DIAGNOSIS	LOCATION	FEATURES
Anterior mediastinal mass	Thyroid mass	Contiguous with thyroid gland	Deviation of trachea
	Thymoma or thymic cyst	Thymic bed	Smoothly marginated
	Lymphoma and small cell lung cancer	All lymph node stations in superior mediastinum, thymic bed, prevascular space, aorticopulmonic window	May be lobulated Mass may involve multiple lymph node groups Hilar lymph node enlargement may be asymmetric
		Extramediastinal location hilar lymph nodes	Hodgkin disease spreads from thymic bed to middle mediastinum to hilar lymph nodes
	Germ cell tumor	Variable, including prevascular space and thymic bed	Fat, hair, and teeth are diagnostic May be homogeneous with smooth margins
Middle mediastinal mass	Duplication cyst (includes bronchogenic cyst)	Most often located at bifurcation of trachea and central airways May be paraesophageal or intraparenchymal	Smoothly marginated High-attenuation fluid
	Lymphadenopathy	All lymph node stations, including subcarinal space	May appear as separate enlarged nodes or as a multiple lymph node mass May be homogeneous or heterogeneous Low attenuation indicates tuberculosis Single site with enhancement indicates Castleman disease
	Pericardial cyst	Adjacent to heart, especially in cardiophrenic sulcus	Smoothly marginated Water attenuation Can also represent pericardial diverticulum if history of mediastinoscopy
	Thyroid mass (intrathoracic goiter)	Thyroid, extending into thorax 15% of these masses extend behind the trachea	Appearance of thyroid tissue is heterogeneous, can include calcifications and focal fluid
	Tracheal tumor	Within or surrounding trachea	Narrowing of trachea Adenoid cystic carcinoma has more tumor outside the trachea than within it, so-called toothpaste lesion
	Vascular variants and abnormalities	Posterior to trachea Anterior or posterior to esophagus	Diverticulum of Kommerall with aberrant subclavian artery Vascular rings and slings
Posterior mediastinal mass	Esophageal abnormalities and masses	Large esophageal mass can occupy middle and posterior mediastinal compartments	Esophageal cancer Foregut duplication cyst
	Neurogenic tumor	Connected to neural foramen	Smoothly marginated or lobulated May have low attenuation May contain fat
	Extramedullary hematopoiesis	Paraspinal masses	Masses are often paired Smoothly marginated

Note: Radiographic division of middle mediastinum may include esophagus, thyroid, and lymph nodes, leaving neurogenic tumors and extramedullary hematopoiesis as primary considerations in posterior mediastinum.

조언

- 사진은 가능성일 뿐이며, 판독은 가능성일 뿐이다
- 사진보다 중요한 것은 증상이다; 사진은 증상보다 뒤늦게 움직인다
- 영상의학과의 판독을 믿지 말아라, 하지만 영상의학과 전문의의 조언은 항상 귀담아 들어야 한다
- 특히 수술 받은 환자의 경우 수술을 이해해야만 정확히 판독이 가능하다
- 수술 후 anatomy는 외과의사만이 제대로 이해가 가능하다

조언

- 영상은 병에 대한 사전 지식이 있어야 해석이 가능하며, 지식을 바탕으로 확률을 계산하는 것이다
- 사진은 항상 이전 사진과 비교해야 한다
- 수술 시 최근 한 달 이내의 사진을 확인해야 한다
- 수술전 항암 방사선 치료를 받은 이후에는 치료 이전과 반드시 비교해야 한다
- 수술 후에는 반드시 수술 전 이미지와 수술 소견을 맞추어 보는 연습을 해야 한다
- 병변은 여러분이 생각하는 곳과 다른 곳에 위치할 수 있다 (특히 폐)

Disease pattern

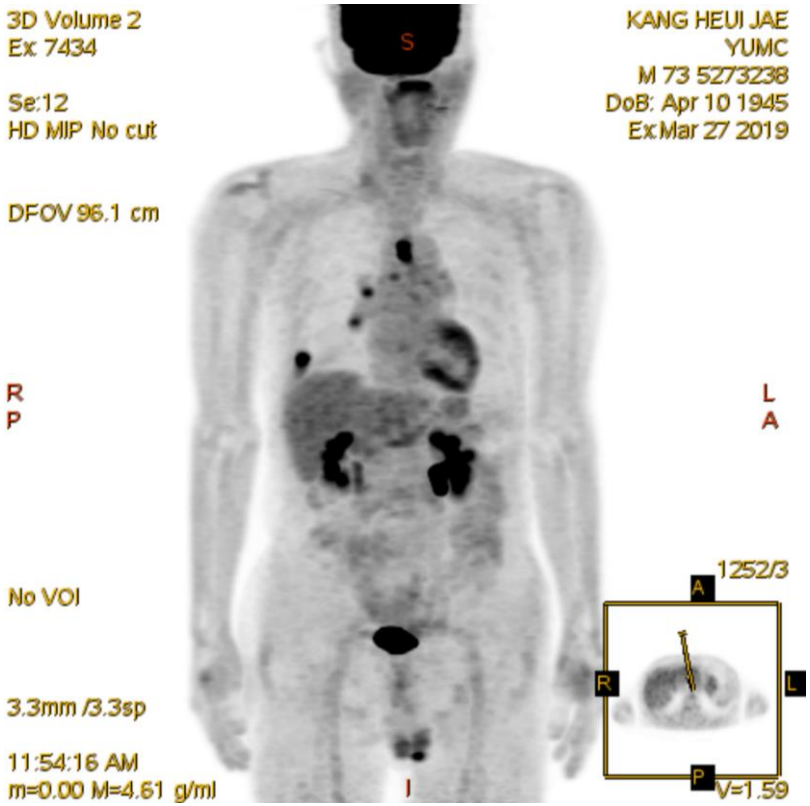

- Intense FDG uptake in the known RLL subpleural nodule, suspicious for primary malignancy.
- Enlarged LNs with intense FDG uptake in the Rt. interlobar, Rt. hilar and Rt. lower paratracheal spaces, suggesting LN metastases.
- Intense FDG uptake in the upper to middle esophagus, suspicious for double primary esophageal cancer. D/Dx> paraesophageal metastatic LNs, less likely; Rec) Enhanced CT and EGD.
- No other remarkable findings.

Bedside Ultrasound

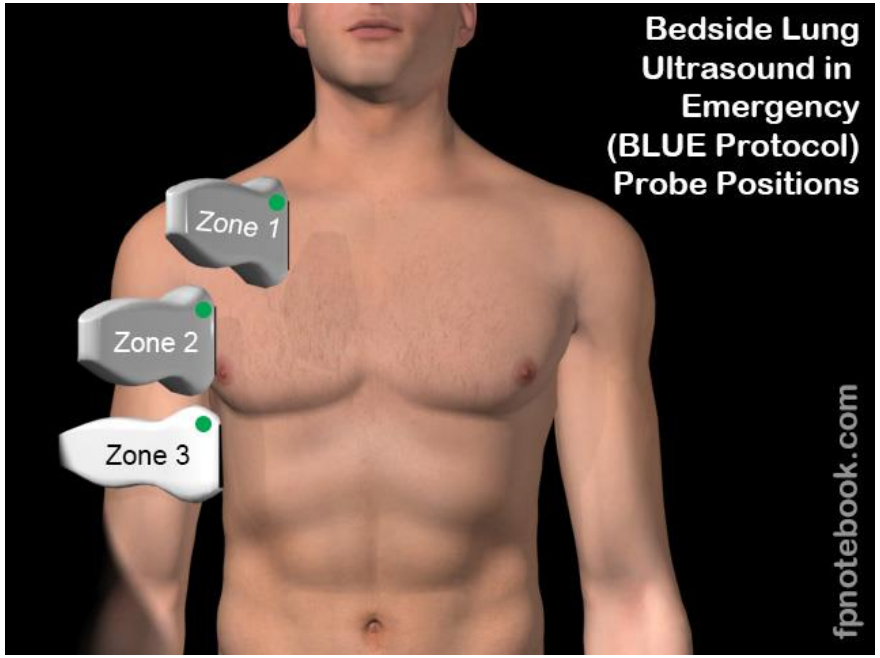

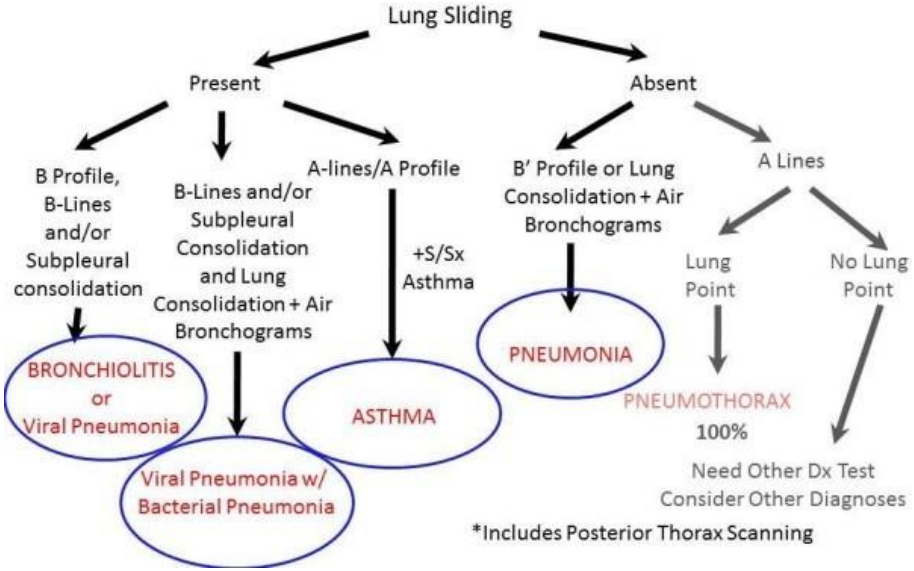

Effusion in ultrasound

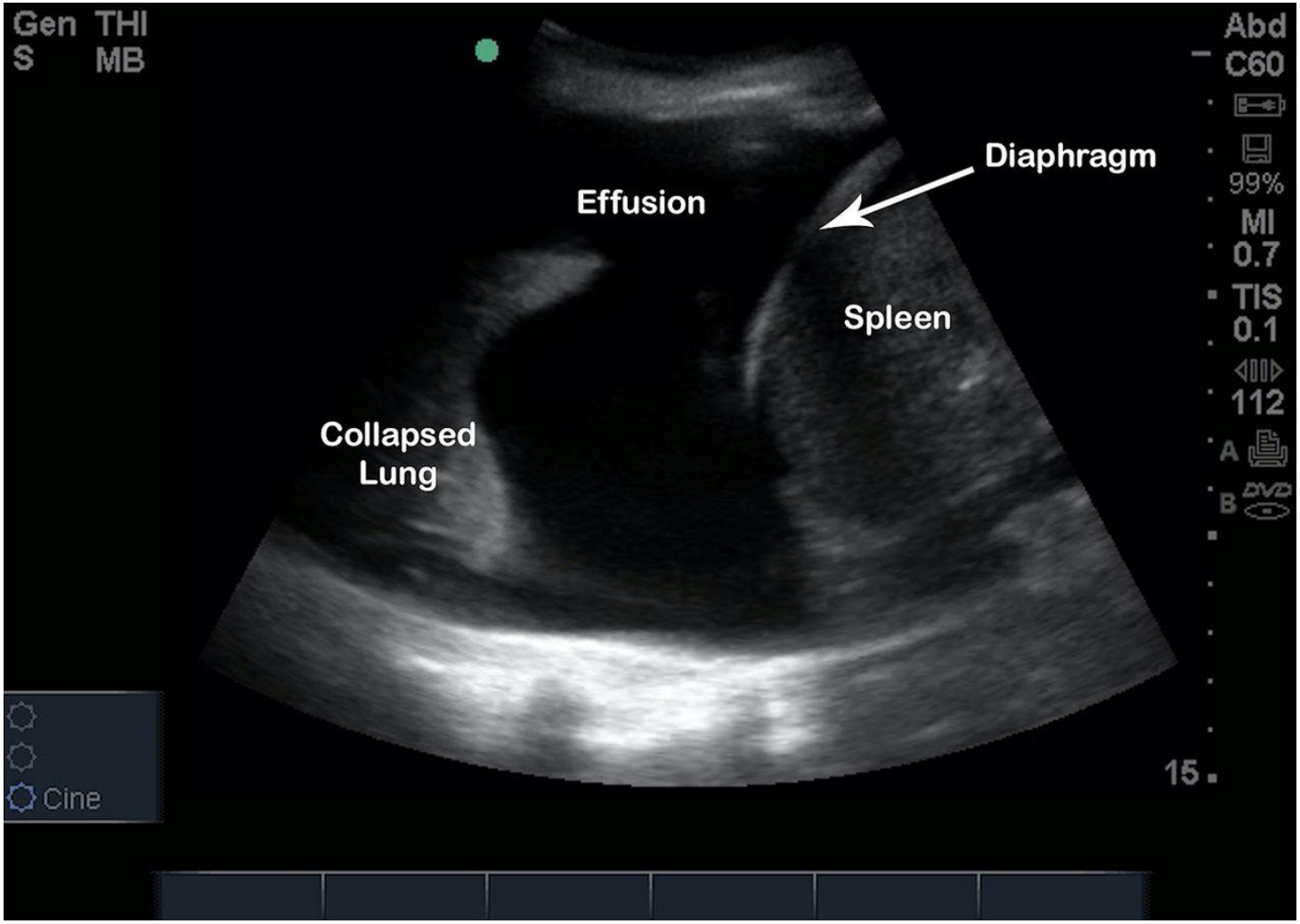

Pneumothorax in ultrasound

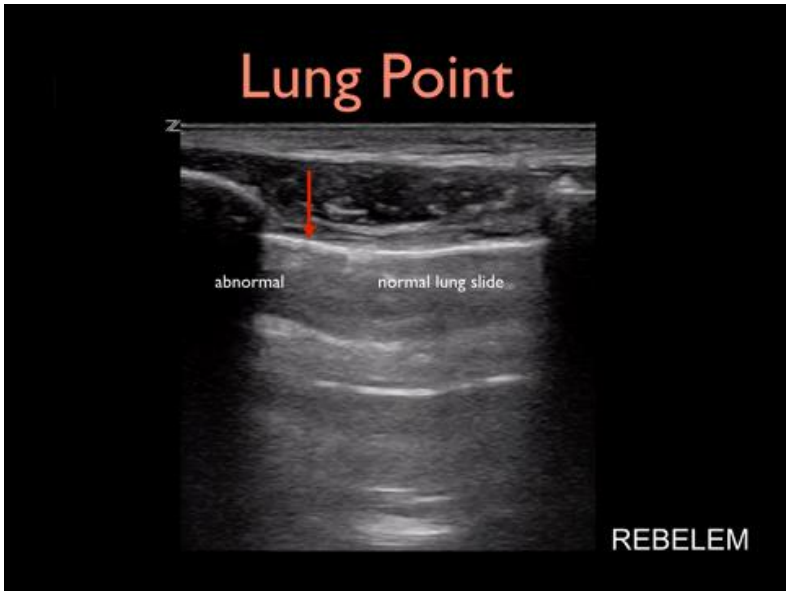

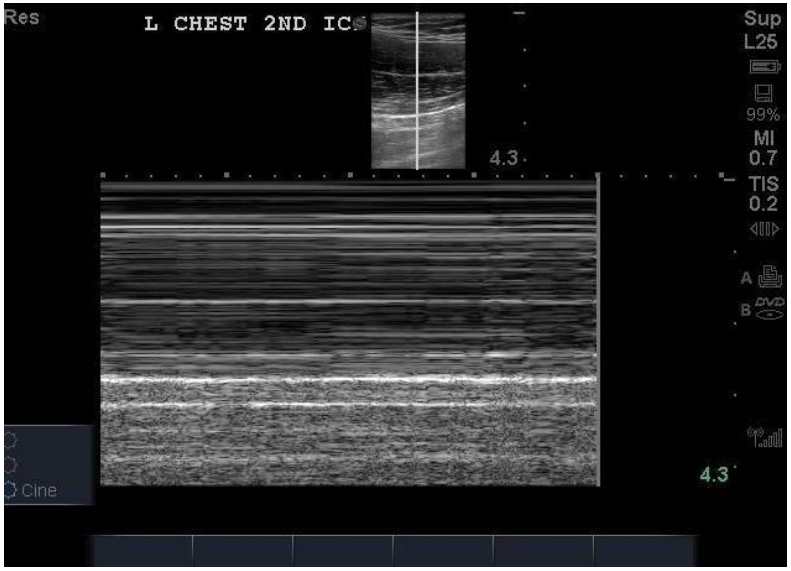

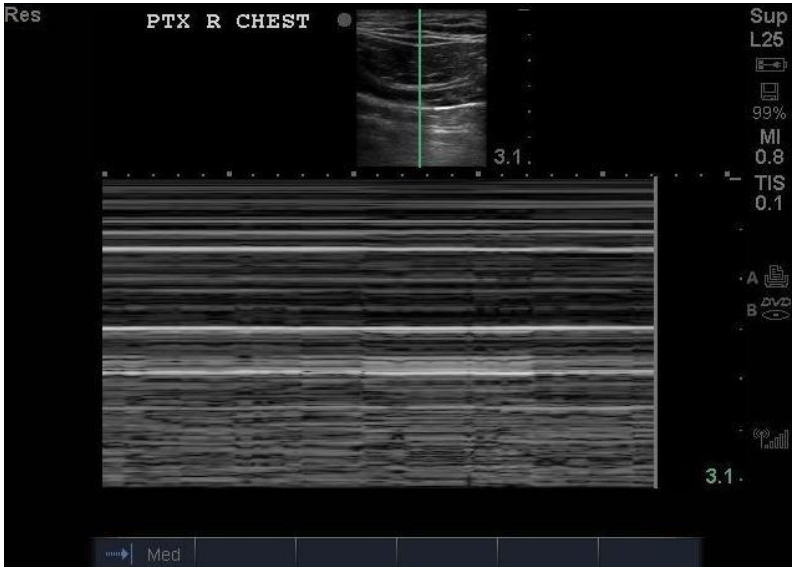


Thank you for attention!!!